



Transport of microplastics in stormwater treatment systems under freeze-thaw cycles: Critical role of plastic density

Vera S. Koutnik^a, Jamie Leonard^a, Jaslyn Brar^a, Shangqing Cao^a, Joel B. Glasman^a, Win Cowger^b, Sujith Ravi^c, Sanjay K Mohanty^{a,*}

^a Department of Civil and Environmental Engineering, University of California, Los Angeles, CA, USA

^b Moore Institute for Plastic Pollution Research, Long Beach, CA, USA

^c Department of Earth & Environmental Science, Temple University, Philadelphia, PA, USA

ARTICLE INFO

Keywords:

Stormwater
Weathering
Plastic pollution
Freezeing
Sand biofilters
Subsurface transport

ABSTRACT

Stormwater treatment systems remove and accumulate microplastics from surface runoff, but some of them can be moved downward to groundwater by natural freeze-thaw cycles. Yet, it is unclear whether or how microplastic properties such as density could affect the extent to which freeze-thaw cycles would move microplastics in the subsurface. To examine the transport and redistribution of microplastics in the subsurface by freeze-thaw cycles, three types of microplastics, with density smaller than (polypropylene or PP), similar to (polystyrene or PS), or greater than (polyethylene terephthalate or PET) water, were first deposited on the top of packed sand—the most common filter media used in infiltration-based stormwater treatment systems. Then the columns were subjected to either 23 h of drying at 22 °C (control) or freeze-thaw treatment (freezing at -20 °C for 6 h and thawing at 22 °C for 17 h) followed by a wetting event. The cycle was repeated 36 times, and the effluents were analyzed for microplastics. Microplastics were observed in effluents from the columns that were contaminated with PET and subjected to freeze-thaw cycles. Comparison of the distribution of microplastics in sand columns at the end of 36 cycles confirmed that freeze-thaw cycles could disproportionately accelerate the downward mobility of denser microplastics. Using a force balance model, we show that smaller microplastics (<50 μm) can be pushed at higher velocity by the ice-water interface, irrespective of the density of microplastics. However, plastic density becomes critical when the size of microplastics is larger than 50 μm. The coupled experimental studies and theoretical framework improved the understanding of why denser microplastics such as PET and PVC may move deeper into the subsurface in the stormwater treatment systems and consequently elevate groundwater pollution risk.

1. Introduction

Terrestrial soil surface and subsurface are major sinks of microplastics in the environment (Li et al., 2021; Nizzetto et al., 2016; Scheurer and Bigalke, 2018) from where they can either move deeper into the ground (Viaroli et al., 2022) or be transported away by wind (Bullard et al., 2021; Rezaei et al., 2019) or stormwater (Piñon-Colin et al., 2020; Werbowski et al., 2021). In particular, stormwater treatment systems remove most microplastics from the surface runoff (Gilbreath et al., 2019; Lange et al., 2021; Smyth et al., 2021), which is a major conveyor of microplastics in the terrestrial environment (Boni et al., 2021; Lutz et al., 2021; Werbowski et al., 2021). These

accumulated microplastics could have several health and environmental impacts (Li et al., 2022; Prata et al., 2020). For instance, airborne microplastics could pose inhalation health risks (Prata, 2018) due to their suspension via wind in agricultural land (Borthakur et al., 2021a), where contaminated biosolids have been applied (Crossman et al., 2020; Koutnik et al., 2021a). Microplastics retained in the subsurface could affect root systems in stormwater and agricultural systems (Chen et al., 2022; Huang et al., 2021; Khalid et al., 2020). Nano- and microplastics could carry some of the pollutants into groundwater aquifers if their mobility in the subsurface is not retarded (Samandra et al., 2022; Zhou et al., 2022). Thus it is critical to understand the processes that affect the mobility of microplastics in subsurface soil including stormwater

* Corresponding author at: Assistant Professor, Department of Civil and Environmental Engineering, The University of California, Los Angeles, 420 Westwood Plaza 5732-C Boelter Hall, Los Angeles, CA, 90095.

E-mail address: mohanty@ucla.edu (S.K. Mohanty).

<https://doi.org/10.1016/j.watres.2022.118950>

Received 11 June 2022; Received in revised form 12 July 2022; Accepted 4 August 2022

Available online 5 August 2022

0043-1354/© 2022 Elsevier Ltd. All rights reserved.

treatment systems.

Accumulated microplastics in stormwater treatment systems could disintegrate into smaller particles by photochemical or biological processes (Sørensen et al., 2021; Zumstein et al., 2018) and move downward during intermittent infiltration of stormwater (Gao et al., 2021; Koutnik et al., 2022a; Mohanty et al., 2015; O'Connor et al., 2019). Subsurface soil naturally experiences dry-wet and freeze-thaw cycles, which could increase the transport of the deposited microplastics (Dong et al., 2022; Gao et al., 2021; Koutnik et al., 2022a; O'Connor et al., 2019). Compared to numerous studies that have examined the mechanism of particle transport by dry-wet cycles (Borthakur et al., 2021b; Gu et al., 2018; Mohanty et al., 2015; O'Connor et al., 2019; Seiphoori et al., 2020), fewer studies have examined the mechanism of particle transport by freeze-thaw cycles (Alimi et al., 2021; Koutnik et al., 2022a; Mohanty et al., 2014). Freeze-thaw cycles could either increase microplastic mobility by disrupting the deposited microplastics during the expansion of the ice crystals (Mohanty et al., 2014) or decrease the mobility by increasing their aggregation (Alimi et al., 2021). Both aggregation and transport in pore water or porous media depend on particle properties such as density, size, and surface properties (Bennacer et al., 2013; Bradford et al., 2003, 2002; Zhang et al., 2014). Yet, none of the previous studies on microplastics examined whether and how the properties of microplastics could determine the extent to which their mobility is affected by the oscillating the ice-water interfaces during freeze-thaw cycles.

Many studies have examined the dynamics of colloids near the freezing interfaces (Asthana and Tewari, 1993; Azouni et al., 1997; Hattori et al., 2020; Körber et al., 1985; Lin et al., 2020; Rempel and Worster, 2001, 1999; Saint-Michel et al., 2017; Shangquan et al., 1992; Tyagi et al., 2020), and they can help explain the behavior of microplastics in the subsurface soil subjected to freeze-thaw cycles. During freeze-thaw cycles, colloids in pore water could experience three types of forces: gravitational force owing to particle size and density, buoyancy owing to the density of the water displaced by the submerged particle, and the interfacial force exerted by moving ice-water interfaces when the interface comes close to within few nanometer distances of the colloid (Azouni et al., 1997; Spannuth et al., 2011; Tyagi et al., 2020). The interfacial force can be sensitive to colloid surface properties (Körber et al., 1985; Shangquan et al., 1992; Thompson and Wettlaufer, 1999). The resulting force balance determines the velocity of colloids near ice front. At a close distance (\sim few nm) between the particle and ice front, the drag force also changes due to the movement of water molecules from bulk to the interface, where the curvature of the ice surface near the particle could change based on the thermal conductivity of the particle (Rempel and Worster, 2001). As microplastics are insulators, they thermally shields the local interface underneath the particle, creating a cooler spot where the ice interface grows faster to create a convex protuberance that could prevent the engulfment of microplastics (Asthana and Tewari, 1993). Thus, convex protuberance could push microplastics and accelerate their mobility in the subsurface. Consequently, the transport of microplastics by these forces could depend on the density, thermal and surface properties of microplastics. Yet, no study to date has examined the effect of microplastic density on their mobility in porous media under freeze-thaw cycles.

The research objectives of the study are: (1) to examine the effect of the density of microplastics on their mobility in the subsurface filter media subjected to freeze–thaw cycles and (2) theoretically estimate the change in velocity of microplastics as a function of their size and density near moving ice-water interfaces in still water, which is typically the case during freezing conditions in the subsurface soil. We hypothesize that freeze-thaw cycles will disproportionately move denser microplastics downward. The rationale behind the hypothesis is that the specific gravity of microplastics could determine whether a plastic particle would sink or float in pore water, and the formation of ice could separate the gap between them by pushing the microplastics up or downward based on the relative position of microplastics with respect to

ice crystal growth. To test the hypothesis, we quantified the mobility of microplastics with different densities in water columns with and without porous media during freeze-thaw cycles and compared the difference in the depth distribution of microplastics as a function of their density following many freeze-thaw cycles. The results could help predict the fate of microplastics in subsurface or stormwater biofilters subjected to freeze-thaw cycles.

2. Materials and Methods

2.1. Microplastics preparation and characterization

We selected three plastic polymers based on their densities lower than (polypropylene or PP, $\rho_{PP} = 920 \text{ kg m}^{-3}$), similar to (polystyrene or PS, $\rho_{PS} = 1,015 \text{ kg m}^{-3}$), and greater than (polyethylene terephthalate or PET, $\rho_{PET} = 1,350 \text{ kg m}^{-3}$) the density of water ($\rho_W = 1,000 \text{ kg m}^{-3}$ at 12°C) (Koutnik et al., 2021b). These three plastic types are commonly used in single-use plastic products and have been extensively found in natural environments and in stormwater (Koutnik et al., 2021b). To create irregular-shaped microplastics, plastic objects made from one of the three types of polymers were abraded using a mechanical orbital sander (Figure S1), following the method described elsewhere (Koutnik et al., 2022a). Sanding created irregularly shaped microplastic particles such as fragments and fibers, similar to what has been found in stormwater (Piñon-Colin et al., 2020).

Microplastics were characterized for their size distribution, shape, and for polymer types using Thermo Scientific Nicolet™ iN10 Fourier Transform Infrared spectroscopy (FTIR) in the reflectance mode using the particle analysis wizard included in the PICTA™ software (Details in Supplementary Materials) (Brahney et al., 2020). FTIR microscope can identify the size distribution of microplastics larger than $20 \mu\text{m}$ in diameter based on the image analysis of particles spread on a 1 cm^2 area of a slide. To analyze the size distribution of microplastics at a wider size range ($0.1 \mu\text{m}$ to 2 mm), we used a laser diffraction particle size analyzer (LS 13320, Beckman Coulter, Inc. CA, USA), where dry microplastics were dispersed by the Tornado Dry Powder System in the chamber before analyzing the diffracted laser beams from microplastics.

The grinding of plastic objects resulted in particles with a range of shapes and sizes. FTIR analysis confirmed that more than 97% of the particles analyzed matched the plastic polymer designated in the plastic object (Figure S2). The shape of the microplastics varied widely from fiber (aspect ratio > 3) to fragment shape (Figure S2). Between 11–20% of the particles created were fibers (Figure S3). The size distribution of the plastic mixtures varied by plastic polymer types (Figure S2). 54% of the PS microplastics were sized between $100 - 250 \mu\text{m}$, whereas a similar majority for PET and PP were sized between $50 - 100 \mu\text{m}$. A laser diffraction analyzer recorded a slightly different size distribution than that observed using an FTIR microscope (Figure S4).

2.2. Sand filter design

Sand is the most common media used in infiltration-based stormwater treatment systems in order to increase the infiltration of surface runoff (Tirpak et al., 2021). Thus, we used quartz sand with sizes between $600\text{--}800 \mu\text{m}$ (20–30 Standard Sand, Certified MTP) packed in transparent PVC columns (2.54 cm in diameter and 30 cm in height) to create model biofilters, similar to a previous study (Koutnik et al., 2022a). Briefly, sand was packed in 2–3 cm increment layers to a total filter media height of 15 cm above the bottom drainage layer, which consisted of glass wool spread on pea gravel at the bottom. The columns were saturated with deionized (DI) water from the bottom, and the pore volume was estimated based on the weight difference between saturated and dry columns. A total of 20 columns were packed to compare the mobility of 3 types of microplastics by either dry-wet (control) or freeze-thaw treatment. Triplicate columns were used per one type of

microplastics per treatment.

2.3. Distribution of microplastics in the water column without porous media during freezing

To simulate the redistribution of suspended microplastics in pore water without being constricted by porous media, we freeze microplastic suspension in a column without porous media. Microplastic suspensions were prepared by mixing a specific amount of each of the three microplastics in 100 mL of DI water in a 1L pre-cleaned glass bottle. The suspension was poured into pre-washed transparent PVC columns, which were placed in a freezer at -15 °C at an up-right position overnight for 18 h. The frozen columns were placed in a warm water bath for 1-2 min to melt ice near the wall and loosen the ice core. The ice core was laid on an aluminum foil and sliced into segments of 3 cm in length with a heated iron knife. Each segment was melted in a clean glass bottle and weighed before filtering the water samples through a 24 mm G4 glass fiber filter paper with 1.2 µm pore size (ThermoFisher Scientific, 09-804-24C) to isolate microplastics in each ice core segment.

2.4. Transport of microplastics in saturated sand columns by freeze-thaw cycles

The transport experiments were conducted following the method outlined elsewhere (Koutnik et al., 2022a). Briefly, packed sand columns were conditioned to remove any colloids or particulates by injecting 4 pore volumes (PV) or ~100 mL of synthetic stormwater at 5 mL min⁻¹ using a peristaltic pump. We used synthetic stormwater (6 mM NaCl) with a similar pH (adjusted) and ionic strength as a natural stormwater collected from Ballona Creek, Los Angeles, USA (Ghavanloughajjar et al., 2020). The use of synthetic stormwater prevented cross-contamination with microplastics and particles typically present in natural stormwater. The effluent samples for each column were collected and analyzed for background microplastic concentration (ranging from 0.01 p mL⁻¹ to 0.18 p mL⁻¹). To simulate microplastic accumulation on biofilters for many years (Koutnik et al., 2022a), 0.1 g of each polymer type of microplastics was deposited on the top of 6 columns, of which 3 columns were subjected to drying treatment (control), and the other 3 columns were subjected to freeze-thaw treatment.

During natural freezing in subsurface, pore water freezes, and water does not typically flow through pores as precipitation occurs via snowfall. During the thawing process, snow melts create runoff, which could pass through the subsurface mobilizing any deposited colloids or microplastics. To simulate microplastic transport during freeze-thaw cycles in nature, the columns were subjected to freeze-thaw cycles followed by infiltration events as described elsewhere (Mohanty et al., 2014). Briefly, the contaminated columns were subjected to 23-h of either drying or freeze-thaw treatment followed by a 20-min injection of 4 PV of synthetic stormwater at 5 mL min⁻¹ or 0.96 cm min⁻¹, which was below the hydraulic conductivity of the packed sand. To simulate freeze-thaw treatment, columns were frozen at -20 °C for 6 h and thawed at 22 °C for 17 h. To simulate drying treatment, the columns were drained by gravity and dried at 22 °C for 23 h. The cycles (drying followed by wetting or freeze-thaw followed by wetting) were repeated 36 times, and the effluents were analyzed for microplastic concentrations after 1, 8, 15, 22, 26, 31, and 36 cycles to estimate potential breakthroughs in deposited microplastics. To account for any microplastics that were already present in the sand before the contamination stage, uncontaminated sand columns were subjected to dry-wet or freeze-thaw cycle treatments, and effluents were analyzed for microplastics.

In the end, all columns were dismantled to sample sand from different depths from specific depths (0.5, 1, 2, 3, 4, 5, 8, 12 cm), starting from the bottom-most depth (near effluent). As straining was found to be a dominant removal process of large microplastics in the stormwater biofilters (Koutnik et al., 2022b), the depth distribution was fitted to an empirical equation (Eq. 1):

$$C(z) = C_0 e^{-Kz} \quad (1)$$

where $C(z)$ and C_0 are microplastic concentrations (p g⁻¹) at depth z (cm) and on the surface respectively, and K is the retardation coefficient. Thus, K is estimated by the fitting depth and concentration data into the model and includes effects of absorption, straining, gravity settling, and removal by any other mechanism.

2.5. Analysis of effluent and filter media samples

To isolate microplastics from effluent, water samples were vacuum filtered through 24 mm glass fiber filter membranes with 1.2 µm pore size (Thermo Fisher Scientific), and the filtered microplastics were stained by adding 0.17 mL of 0.5 µg mL⁻¹ Nile Red in chloroform solution on filters inside a glass petri dish (Koutnik et al., 2022b). Filters were air-dried with a glass cover and imaged using a smartphone-based fluorescence microscope. The details of the method is described elsewhere (Leonard et al., 2022), which has been used in multiple studies with environmental and laboratory samples (Koutnik et al., 2022a, 2022b). The method permits the counting of microplastics that can adsorb Nile Red dyes and does not differentiate between different types of plastic polymers. To estimate the concentration of microplastics retained at different depths of the sand filters, 1 g of oven-dried sand sample was mixed in 40 mL of 1.6 g mL⁻¹ KI solution in a 50 mL centrifuge tube, and the mixture was centrifuged at 5000 rpm for 30 min to settle sand particles, leaving the lighter (density < 1.6 g cm⁻³) particles including microplastics to float on the supernatant surface (Mu et al., 2019). The supernatant was filtered to isolate plastics, stained using Nile Red, and analyzed for microplastic concentration as described earlier. The concentrations were reported as the number per L of effluent or g of filter media. To analyze the difference and similarity between the measured concentrations between contaminated plastic or treatment types, we performed a Wilcoxon rank-sum test (R version 4.0.0).

2.6. Quality assurance and quality control

All lab surfaces were wiped down every day and before and after usage. Samples were collected, stored, and processed using pre-washed laboratory glassware. All glassware and containers were washed with soap and water and then rinsed with DI water three times to remove any background microplastics. Glass covers or clean aluminum foil were used to prevent airborne contamination during the sample processing. Uncontaminated filter media was analyzed from each column depth for any background concentration of microplastics, which was subtracted from the concentration of microplastics at the same depth in contaminated columns to estimate the true penetration depth of added microplastics. The DI water used in this study was analyzed for possible microplastic contamination. The contributions of microplastics from plastic tubing for pumping, PVC plastic columns, centrifuge polypropylene test tubes, and plastic pipette tips were estimated using appropriate blanks. During every day of analysis, a method blank was run, following the same lab procedure. The mean of laboratory blanks for each method was subtracted from the measured concentration of samples to account for any microplastics introduced from procedural steps.

3. Results

3.1. Distribution of microplastics in frozen water columns without porous media

The redistribution of microplastics in pore water during freeze-thaw cycles could depend on the force exerted by the moving ice-water interface and physical constraints from the surface porous media near the pore water. Analysis of the distribution of microplastics in frozen

water columns without sand media revealed that microplastic distribution in pore water with the constraint of porous media varied with microplastic density (Fig. 1). More than 60% of PP microplastics were found at the surface, with their concentration decreasing with depth. In contrast, PET concentration was higher at lower depths. About 20% of PET particles were found at the surface despite being expected to sink due to their greater density than water.

3.2. Distribution of microplastics in sand columns subjected to freeze-thaw cycles

Depth distribution of microplastics in columns packed with sand showed that freeze-thaw cycles increased the penetration depth of microplastics compared to dry-wet cycles (Fig. 2). Irrespective of treatment methods, the downward mobility was more pronounced for denser microplastics such as PET. The distribution was sensitive to the density of microplastics. For all the columns subjected to dry-wet cycles, the microplastic concentration near the outlet was similar to the background concentration ($0 - 7 \text{ p g}^{-1}$) irrespective of microplastic density. In contrast, for the columns subjected to freeze-thaw treatments, microplastic concentration near the outlet was similar to background concentration only for columns contaminated with two types of plastics: PP and PS. Regardless of the weathering, PET microplastics moved deeper into columns than the PP and PS particles.

Fitting the distribution of microplastics with the exponential model (Equation 1) (Koutnik et al., 2022b, 2022a), we showed that retardation of microplastics in sand biofilters varied with microplastic density irrespective of treatment types, but the density had a more pronounced effect on microplastic retardation under freeze-thaw cycles than that under dry-wet cycles (Fig. 2). Specifically, the retardation coefficient, which is estimated based on the slope of the graphs in Figure 2C-D, ranges from 1.1 to 5.5, with the highest slope corresponding to PET in columns subjected to freeze-thaw cycles.

3.3. The concentration of microplastics in the effluent

Analysis of microplastic concentration in the effluent from all columns revealed that transport of PP and PS microplastics was negligible and statistically insignificant irrespective of the treatment types (Fig. 3). The 15-cm deep sand media was sufficient to prevent the transport of PP and PS microplastics out of the columns via effluent. In contrast, PET microplastics were found in higher concentrations than the background

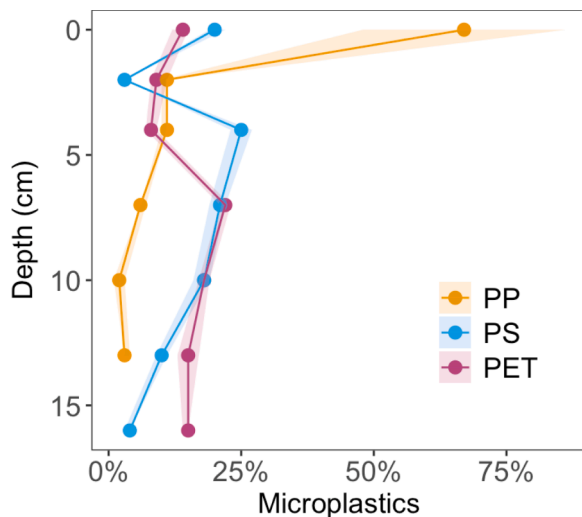


Figure 1. Fraction of total microplastics in water found at each depth of the frozen water column for three plastic polymer types: polypropylene (PP), polystyrene (PS), and polyethylene terephthalate (PET). The shaded area shows a 95% confidence interval due to the variance between multiple measurements.

concentration from uncontaminated or blank columns. The background concentrations were 0.023 p mL^{-1} and 0.075 p mL^{-1} for blank columns with dry-wet and freeze-thaw cycles, respectively. The higher effluent concentration of PET microplastics in contaminated columns subjected to freeze-thaw cycles further confirmed the finding that PET microplastics were disproportionately moved by freeze-thaw cycles.

4. Discussion

4.1. Retention of microplastics in sand columns.

All deposited microplastics, with the exception of PET microplastics in columns subjected to freeze-thaw cycles, were retained in sand columns. Among the three types of microplastics used, PET is heavier than water. Freeze-thaw treatment decreased the retention of PET microplastics and enhanced their mobility more than that of PP and PS microplastics. The results indicate that in most conditions, microplastics with densities lighter than water can be effectively retained in the subsurface. The results are similar to previous studies that showed the removal of microplastics in sand columns (Gao et al., 2021; Koutnik et al., 2022a; O'Connor et al., 2019; Rong et al., 2022; Waldschläger and Schüttrumpf, 2020). Most microplastics were removed in sand columns due to the physical straining (Koutnik et al., 2022b, 2022a), which is sensitive to the size of microplastics and pore size of the media (Bradford et al., 2003). Straining occurs when larger particles are blocked by the narrow pores (Auset and Keller, 2006). PS particles used in this study were larger than PE or PET particles (Figure S2). Therefore, PS microplastics are expected to be removed by sand by straining to a greater extent than the other two types of microplastics. Larger microplastics blocked at narrow pore throats between sand grains could not move further, irrespective of dry-wet or freeze-thaw cycles. This partially explained why PS microplastics were retained to a greater extent than the other two types of microplastics irrespective of weathering treatments.

Among plastic types, PET microplastics were found in greater concentration than the background level in the effluents of columns subjected to freeze-thaw cycles (Fig. 3). The depth distribution data (Fig. 2) also confirmed the enhanced mobility of PET microplastics by freeze-thaw cycles. The result indicates that the density of microplastics plays a critical role in the remobilization of microplastics by freeze-thaw cycles compared to dry-wet cycles. Previous studies (Mohanty et al., 2015, 2014) have compared the remobilization colloids by dry-wet and freeze-thaw cycles, but they did not vary the density of colloids. Chrysikopoulos and Syngouna (2014) examined the role of gravity on the transport of colloids in sand columns by comparing the transport of bacteria (specific gravity similar to PET ~ 1.4), and natural clay colloids (specific gravity ~ 2.6) and observed that an increase in specific gravity of colloid increased in colloid transport velocity in vertical sand columns. Collectively, the results confirmed that denser colloids are more susceptible to transport than lighter colloids.

4.2. Enhanced transport of microplastics by freeze-thaw cycles compared to dry-wet cycles

For the same microplastic type, freeze-thaw cycles transported more microplastics to the deeper layers than dry-wet cycles did within the columns (Fig. 2). Although the same amount of microplastics was added to all columns, the concentration of microplastics in the top layer of columns subjected to freeze-thaw cycles was slightly higher than the concentration in the top layer of columns subjected to dry-wet cycles. In contrast, the concentration in deeper layers was disproportionately greater in columns with freeze-thaw cycles than in columns with dry-wet cycles. This result agreed with a previous study that compared the transport of PP microplastics in sand and soil columns under dry-wet or freeze-thaw cycles (Koutnik et al., 2022a). Our study provides additional evidence that the effect of the density of microplastics on the transport of

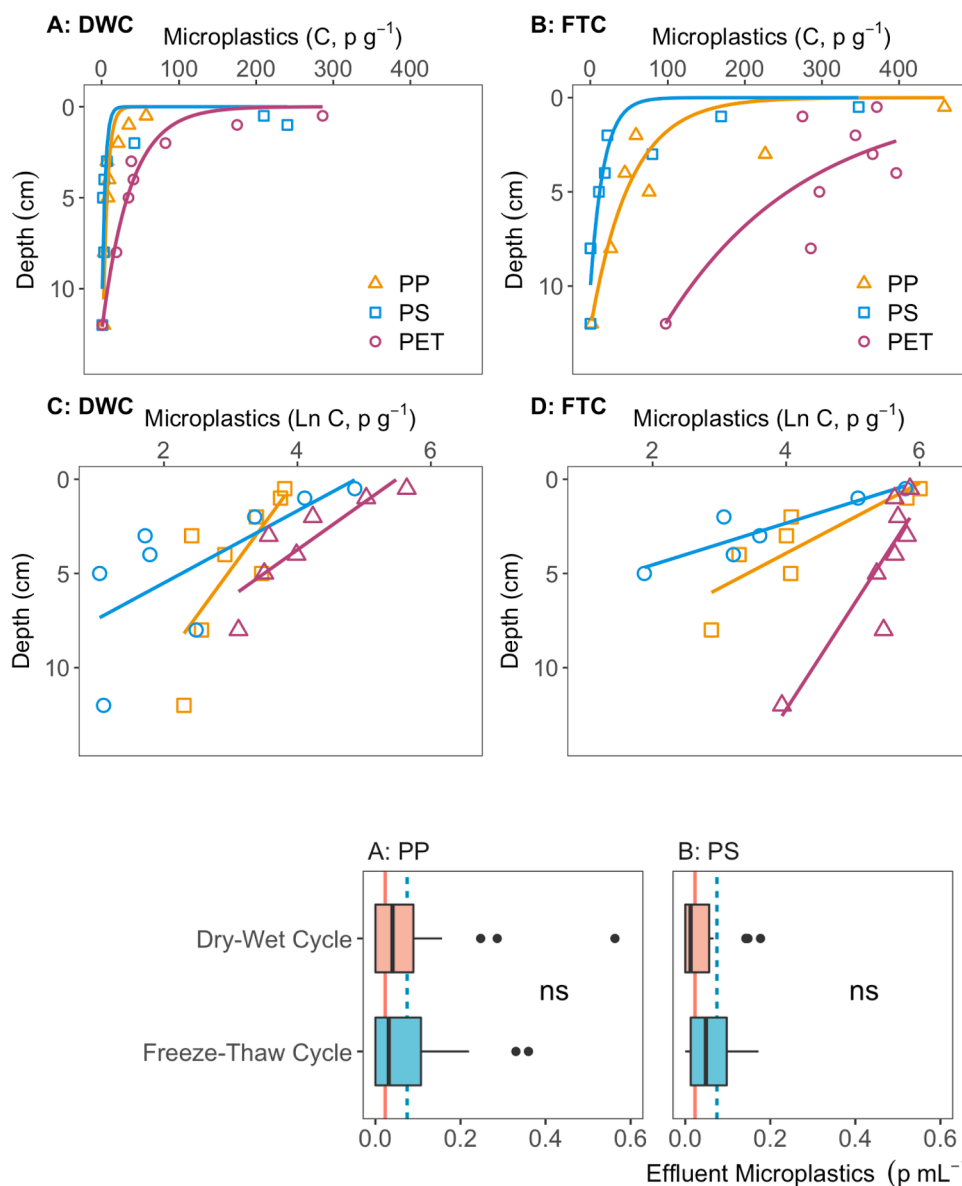


Figure 2. Microplastics concentration by depth for columns contaminated with three types of plastics subjected to either (A,C) dry-wet cycles or (B,D) freeze-thaw cycles. Each point represents an average of the experiment data points between three columns, and the lines represent best fitting exponential model (Equation 1). C and D showing logarithmic concentration of microplastics varying with depth and weathering. The fitted equations and R^2 for each line are provided in Table S2.

Figure 3. Concentration of (A) PP, (B) PS, and (C) PET microplastics in the effluent of the columns subjected to dry-wet cycles and freeze-thaw cycles. ns and * indicate no statistical difference and significant statistical difference with $p < 0.05$, respectively. The solid and dashed vertical lines correspond to the background concentrations of the effluent from control samples for columns subjected to dry-wet and freeze-thaw treatments, respectively.

microplastics during freeze-thaw cycles. In particular, the effect of freeze-thaw cycles is more pronounced for denser microplastics. We attributed the results to fundamental differences in processes by which dry-wet or freeze-thaw cycles could mobilize deposited microplastics in porous media. Advancing or receding wetting fronts during dry-wet cycles typically disrupt solid-water and air-water interfaces where colloids were typically deposited (DeNovio et al., 2004). Thus, the shear force of the rapidly moving air-water interfaces could scour microplastics or colloids from their deposited locations and mobilize them into pore water (Flury and Aramrak, 2017; Shang et al., 2008). The interaction of air-water interfaces on colloids depends on the hydrophobicity of colloids (Keller and Auset, 2007). Thus, hydrophobicity of microplastics may play a greater role than density in the remobilization of microplastics by dry-wet cycles. In contrast to dry-wet cycles, freeze-thaw cycles involve the transition of the water phase to ice. During freezing, deposited microplastics can either be pushed or engulfed by the ice front based on the free energy change to replace particle-liquid (pl) and liquid-solid (lp) interfaces with a solid-particle (sp) interface (Asthana and Tewari, 1993; Shangguan et al., 1992). Ice

front engulfs the particle if the free energy change is negative. As all plastics are insulators, which block the heat energy from water to ice near the interface, the ice formation could accelerate near the microplastics, creating a convex-shaped interface that would be more likely to push microplastics along the direction of ice-interface propagation (Asthana and Tewari, 1993). A moving ice front can be more disruptive than rewetting of the pore by liquid water because expanding ice during freezing can exert more pressures than capillary pressures on pore walls during drying (Koutnik et al., 2022a; Mohanty et al., 2014). The ice crystals can also fracture or expand the pore walls, thereby creating flow paths conducive to the transport of large colloids (Borthakur et al., 2021b).

4.3. Mechanisms of microplastic transport by freeze-thaw cycles

Our results confirmed that the extent to which freeze-thaw cycles could accelerate the downward mobility of microplastics is dependent on the density of microplastics. However, the microplastics used in our study are $>50 \mu\text{m}$, and the detection method used in our study could not

reliably detect microplastics $< 10 \mu\text{m}$. To understand the effect of density on the mobility of microplastics within all size ranges ($0.1 \mu\text{m}$ to $1000 \mu\text{m}$), we estimated the velocity of suspended plastic particles with a spherical shape at far and close (within a few nm) distances from the moving ice interface using a force balance approach (Shangguan et al., 1992). The model does not account for the effect of shape, which is expected to affect the drag force. Furthermore, the model does not account for the interception of microplastics in porous media when pushed by ice and assumed all microplastics were initially present in one location before being separated by different forces described as follows. Consequently, the model could not directly validate the experimental data. Nevertheless, the simplistic model illustrates the importance of microplastic density on their transport in pore water. The velocity of a plastic particle (V_p) far from the moving ice-water interface, as shown in Equation 2, can be derived by force balance where the gravitational force based on the density difference between particle and water ($F_G = \frac{4}{3} \pi R_p^3 \Delta\rho g$) acts against the drag force ($F_D = 6 \pi \mu R_p V_p$). Here, $\Delta\rho$ is the difference in the density of the particle (ρ_p) and water (ρ_L), μ is the viscosity of water, g is the acceleration due to gravity, and R_p is the radius of the particle.

$$V_p = \frac{2}{9} R_p^2 \Delta\rho g \mu^{-1} \quad (2)$$

The particle moves at constant flotation velocity in a direction based on the sign of $\Delta\rho$ (Fig. 4-C). Thus, most PP microplastics are expected to float and stay near the surface of the water column, whereas most PET microplastics are expected to settle at the bottom of columns after sufficient time has passed. Our results (Fig. 1) confirmed the overall trend: more than 60% PP microplastics and less than 15% PET microplastics moved to the top of the water column after freeze-thaw cycles. As the initial position of microplastics in a well-mixed suspension and the time taken to freeze the water column was unknown, Stoke's law could not be used to predict the occurrence of the microplastics present at different depths.

The force balance on the suspended microplastics would change at

close proximity (within a few nanometers) to the ice-water interface, where molecular interactions become relevant. If the particle is denser than water, the interaction between the particle and ice interface would occur only if the velocity of the ice-water interface (V_S) is greater than the settling velocity (V_p) (Fig. 4-A). At a distance of the order of the atomic spacing, the particle would experience an interfacial molecular force (F_i) or the Van der Waals force or the force due to a change in the interfacial energy. In this case, the standard Stokes' equation for the drag force is no longer valid as the flow of liquid is perturbed by the ice front. At this close proximity, the particle experiences a drag force or cryosuction force (F_μ) because water moves from the suspension towards the interface to support ice growth, thereby attracting the particle towards the interface (Fig. 4-A). At equilibrium, the net force on the particle would be zero ($F_G + F_i - F_\mu = 0$) as shown in Equation 3:

$$\frac{4}{3} \pi R_p^3 \Delta\rho g + 2 \pi R_p \Delta\sigma_0 \left(\frac{a_0}{a_0 + d} \right)^n \alpha - 6 \pi \mu V_p^* \frac{R_p^2}{d} \alpha^2 = 0 \quad (3)$$

where a_0 is the sum of the radii of atoms in the surface layers of the particle and the solid, d is the gap between particle and ice-water interface, and $\Delta\sigma_0$ ($= \sigma_{SP} - \sigma_{LP} - \sigma_{SL}$) is the net free energy changes for the particle to be engulfed by ice, which occurs when free energy between the ice and particle (σ_{SP}) exceeds the free energy between water and particle (σ_{LP}), and ice and water (σ_{SL}). α is a function of the curvature of the ice-water interface near the particle, which is the ratio of the radius of curvature of the ice-water interface (R_i) and the difference between the radius of interface curvature and particle radius ($R_i - R_p$). As the curvature is created by the melting of ice due to a difference in thermal conductivity of water and plastic particle, α can be calculated as the ratio of thermal conductivity of particle (k_p) and water (k_L). As the thermal conductivity of microplastics is smaller than water, a convex shape ice hump would form near the interface between the particle and ice, which can push microplastics further. Solving Equation 4, the velocity of the particle near the ice-water interface would become:

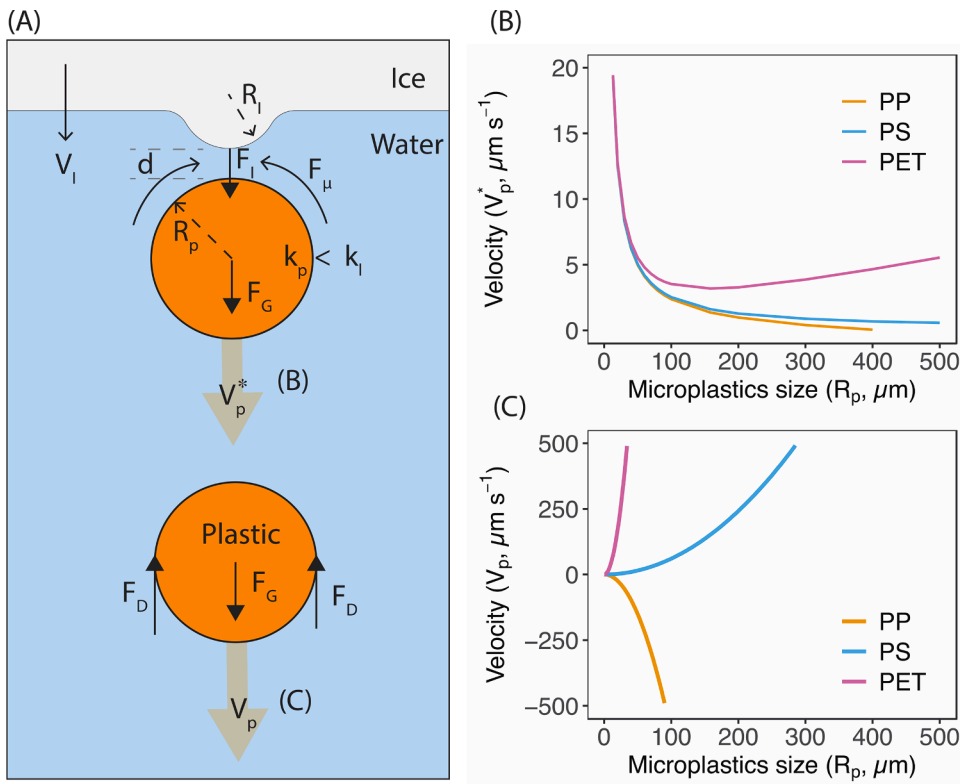


Figure 4. (A) Force balance on microplastic particles near (\sim few nm) and far from the moving ice-water interface. In water away from the ice-water interface, microplastics experience a gravitational force (F_G) based on the density difference between the particle and water and the drag force (F_D) against the direction of movement. At close proximity to the ice-water interface, microplastics would experience an interfacial molecular force (F_i) or the Van der Waals force or the force due to a change in the interfacial energy and a drag force or cryosuction force (F_μ) because water moves from the suspension towards the interface to support ice growth. (B) The velocity of suspended microplastics away from the ice interface using Stokes' law. (C) The velocity of particles near the ice interface. The velocity of microplastics from three polymer types at the interface was calculated using the following assumption: $a_0 = 0.2 \text{ nm}$; $d = 1 \text{ nm}$; $n = 2$; $\Delta\sigma_0 = 10 \text{ mN/m}$; $\mu = 0.0018 \text{ N s/m}^2$, $\rho_{PP} = 920 \text{ kg m}^{-3}$, $\rho_{PS} = 1,015 \text{ kg m}^{-3}$, $\rho_{PET} = 1,350 \text{ kg m}^{-3}$, $\rho_{H_2O} = 1,000 \text{ kg m}^{-3}$, $k_p \text{ or } H_2O = 0.561$, and $k_p = 0.115$.

$$V_p^* = \frac{d}{3\mu\alpha} \left(\frac{\Delta\sigma_0}{R_p} \left(\frac{a_0}{a_0 + d} \right)^n + \frac{2R_p (\rho_p - \rho_L) g}{3\alpha} \right) \quad (4)$$

Estimating the velocity of plastic particles with a radius between 0.1 to 1000 μm near the ice-water interface, we show that the velocity is sensitive to plastic density if the size of microplastic is bigger than 10 μm (Fig. 4-B). The contribution of interfacial force on microplastic mobility was prominent when the particle size was smaller than 10 μm . However, our method is inadequate to detect microplastics within these size ranges. Thus, the velocity of smaller microplastics (< 10 μm) is expected to increase dramatically with a decrease in size due to push from the ice interface irrespective of the density of microplastics. In contrast, the velocity of larger microplastics, such as the ones used in this study, would be much small near the ice-water interface, and the velocity would be affected by the density of microplastics. The theoretical prediction that PET velocity would be much higher than PP and PS near the ice interface is confirmed by our experimental data, where PET microplastics were relocated deeper into the water columns (Fig. 1) followed by PS and PET. Most PP particles were expected to float on the surface, so they were not affected by ice propagation from top to bottom of the columns.

4.4. Environmental Implications

The results of this study provide the first quantitative and experimental evidence showing accelerated transport of microplastics by freeze-thaw cycles as a function of the particle density. The theoretical framework provided here can be applied across all plastic polymers with other densities. Understanding the effects of freeze-thaw cycles is critical due to the prevalence of these seasonal weather patterns across all of northern America and Europe. Furthermore, these results are useful to predict microplastic movement in freshwater lakes or ponds that undergo freezing during winter. As freezing cycles and conditions are expected to vary during climate changes, the results can later be used to understand a change in microplastic distribution in the subsurface under different climates. Predicted climate change scenarios suggest an increase in the frequency and severity of soil freeze-thaw cycles in many northern temperate regions of the world (Henry, 2008), with implications for the subsurface transport rates of different emerging contaminants including microplastics. The results can also help predict microplastic distribution in the soil in the agricultural fields and urban areas and the potential transport pathways to the groundwater (Henry, 2008; Pauli et al., 2013). Although sand was used in this study to demonstrate the impact of freezing and density, the trend is expected to be similar in soils as shown in a previous study (Koutnik et al., 2022a). However, the effect of density or freeze-thaw cycles can be less apparent if most microplastics are removed by straining in narrow flow paths in soil. Thus, soil pore size distribution should be taken into account to accurately determine the effect of microplastic density on their mobility in soil subjected to freeze-thaw cycles. Nevertheless, understanding how far some microplastics would move near the root zone can help predict their impact on root function or crop productivity (Boots et al., 2019; de Souza Machado et al., 2019). Plants growing in microplastic-contaminated soils are predicted to have decreased nutrient contents and increased toxicity as nano plastics can be uptaken by plant roots and soil microbiota (Li et al., 2020; Seeley et al., 2020; Sun et al., 2021). Downward migration also has the potential for groundwater contamination, which serves as a source of fresh water for at least two billion people worldwide (Panno et al., 2019; Samandra et al., 2022; Viaroli et al., 2022). Recent anecdotal evidence showed a greater abundance of denser plastics such as PET and PVC in the groundwater samples, but the cause of such abundance was unknown (Samandra et al., 2022). Our study provided a theoretical basis to predict the increased abundance of denser microplastics in deeper subsurface soil or groundwater aquifers.

5. Conclusions

Based on the experimental evidence and theoretical framework, we proved that the density of microplastics could play a critical role in the transport of microplastics in subsurface soil or other porous media in stormwater treatment systems subjected to natural freeze-thaw cycles. Most microplastics were retained in sand columns, potentially by physical straining if their particle size is larger than the pore size. Based on the force balance calculation on microplastics near the downward moving ice-water interface, smaller microplastics (<50 μm) could be pushed at higher velocity by the ice-water interface, irrespective of the density of microplastics. However, density becomes critical when the size of microplastics becomes larger than 50 μm . For these large microplastics, PET moved deeper into the sand layer compared to low-density microplastics such as PP and PS. These results suggest that among all accumulated microplastics in stormwater treatment systems, denser microplastics such as PET and PVC are more likely to move deeper into the subsurface to groundwater.

Declaration of Competing Interest

The authors declare that they have no known competing financial interests or personal relationships that could have appeared to influence the work reported in this paper.

Data Availability

Data will be made available on request.

Acknowledgments

The authors are grateful for the financial support provided by the UCLA Samueli Engineering School and the UCLA Department of Civil & Environmental Engineering, USA. VSK was partially supported by a fellowship from the US NSF NRT-INFES: Integrated Urban Solutions for Food, Energy, and Water Management program (Grant No. DGE-1735325). JL is supported by the National Science Foundation Graduate Research Fellowship Program (Grant No. DGE-2034835). Any opinions, findings, conclusions or recommendations expressed in this material are those of the author(s) and do not necessarily reflect the views of the National Science Foundation. WC and the FTIR were funded by the McPike Zima Charitable Foundation.

Supplementary materials

Supplementary material associated with this article can be found, in the online version, at doi:10.1016/j.watres.2022.118950.

References

- Alimi, O.S., Farner, J.M., Tufenkji, N., 2021. Exposure of nanoplastics to freeze-thaw leads to aggregation and reduced transport in model groundwater environments. *Water Res* 189, 116533. <https://doi.org/10.1016/j.watres.2020.116533>.
- Asthana, R., Tewari, S.N., 1993. The engulfment of foreign particles by a freezing interface. *J. Mater. Sci.* 28, 5414–5425. <https://doi.org/10.1007/BF00367810>.
- Auset, M., Keller, A.A., 2006. Pore-scale visualization of colloid straining and filtration in saturated porous media using micromodels. *Water Resour. Res.* 42 <https://doi.org/10.1029/2005WR004639>.
- Azouini, M.A., Casses, P., Sergiani, B., 1997. Capture or repulsion of treated nylon particles by an ice-water interface. *Colloids Surf. Physicochem. Eng. Asp.* 122, 199–205. [https://doi.org/10.1016/S0927-7757\(96\)03747-8](https://doi.org/10.1016/S0927-7757(96)03747-8).
- Bennacer, L., Ahfir, N.-D., Bouanani, A., Alem, A., Wang, H., 2013. Suspended particles transport and deposition in saturated granular porous medium: particle size effects. *Transp. Porous Media* 100, 377–392. <https://doi.org/10.1007/s11242-013-0220-4>.
- Boni, W., Arbuckle-Keil, G., Fahrenfeld, N.L., 2021. Inter-storm variation in microplastic concentration and polymer type at stormwater outfalls and a bioretention basin. *Sci. Total Environ.*, 151104 <https://doi.org/10.1016/j.scitotenv.2021.151104>.

- Boots, B., Russell, C.W., Green, D.S., 2019. Effects of Microplastics in Soil Ecosystems: above and Below Ground. *Environ. Sci. Technol.* 53, 11496–11506. <https://doi.org/10.1021/acs.est.9b03304>.
- Borthakur, A., Leonard, J., Koutnik, V.S., Ravi, S., Mohanty, S.K., 2021a. Inhalation risks from wind-blown dust in biosolid-applied agricultural lands: Are they enriched with microplastics and PFAS? *Curr. Opin. Environ. Sci. Health*, 100309. <https://doi.org/10.1016/j.coesh.2021.100309>.
- Borthakur, A., Olsen, P., Dooley, G.P., Cranmer, B.K., Rao, U., Hoek, E.M.V., Blotvogel, J., Mahendra, S., Mohanty, S.K., 2021b. Dry-wet and freeze-thaw cycles enhance PFOA leaching from subsurface soils. *J. Hazard. Mater. Lett.* 2, 100029. <https://doi.org/10.1016/j.hazl.2021.100029>.
- Bradford, S.A., Simunek, J., Bettahar, M., van Genuchten, M.Th., Yates, S.R., 2003. Modeling colloid attachment, straining, and exclusion in saturated porous media. *Environ. Sci. Technol.* 37, 2242–2250. <https://doi.org/10.1021/es025899u>.
- Bradford, S.A., Yates, S.R., Bettahar, M., Simunek, J., 2002. Physical factors affecting the transport and fate of colloids in saturated porous media. *Water Resour. Res.* 38. <https://doi.org/10.1029/2002WR001340>, 63-1-63-12.
- Brahney, J., Hallerud, M., Heim, E., Hahnberger, M., Sukumaran, S., 2020. Plastic rain in protected areas of the United States. *Science* 368, 1257–1260. <https://doi.org/10.1126/science.aaz5819>.
- Bullard, J.E., Ockelford, A., O'Brien, P., McKenna Neuman, C., 2021. Preferential transport of microplastics by wind. *Atmos. Environ.* 245, 118038. <https://doi.org/10.1016/j.atmosenv.2020.118038>.
- Chen, G., Li, Y., Liu, S., Junaid, M., Wang, J., 2022. Effects of micro(nano)plastics on higher plants and the rhizosphere environment. *Sci. Total Environ.* 807, 150841. <https://doi.org/10.1016/j.scitotenv.2021.150841>.
- Chrysikopoulos, C.V., Syngouna, V.I., 2014. Effect of gravity on colloid transport through water-saturated columns packed with glass beads: modeling and experiments. *Environ. Sci. Technol.* 48, 6805–6813. <https://doi.org/10.1021/es501295n>.
- Crossman, J., Hurley, R.R., Futter, M., Nizzetto, L., 2020. Transfer and transport of microplastics from biosolids to agricultural soils and the wider environment. *Sci. Total Environ.* 724, 138334. <https://doi.org/10.1016/j.scitotenv.2020.138334>.
- de Souza Machado, A.A., Lau, C.W., Kloas, W., Bergmann, J., Bachelier, J.B., Faltin, E., Becker, R., Görlich, A.S., Rillig, M.C., 2019. Microplastics Can Change Soil Properties and Affect Plant Performance. *Environ. Sci. Technol.* 53, 6044–6052. <https://doi.org/10.1021/acs.est.9b01339>.
- DeNovio, N.M., Saiers, J.E., Ryan, J.N., 2004. Colloid movement in unsaturated porous media: recent advances and future directions. *Vadose Zone J.* 3, 338–351. <https://doi.org/10.2136/vzj2004.0338>.
- Dong, S., Zhou, M., Su, X., Xia, J., Wang, L., Wu, H., Suakollije, E.B., Wang, D., 2022. Transport and retention patterns of fragmental microplastics in saturated and unsaturated porous media: A real-time pore-scale visualization. *Water Res.* 214, 118195. <https://doi.org/10.1016/j.watres.2022.118195>.
- Flury, M., Aramrak, S., 2017. Role of air-water interfaces in colloid transport in porous media: a review. *Water Resour. Res.* 53, 5247–5275. <https://doi.org/10.1002/2017WR020597>.
- Gao, J., Pan, S., Li, P., Wang, L., Hou, R., Wu, W.-M., Luo, J., Hou, D., 2021. Vertical migration of microplastics in porous media: Multiple controlling factors under wet-dry cycling. *J. Hazard. Mater.* 419, 126413. <https://doi.org/10.1016/j.jhazmat.2021.126413>.
- Ghavanloughaj, M., Valenca, R., Le, H., Rahman, M., Borthakur, A., Ravi, S., Stenstrom, M.K., Mohanty, S.K., 2020. Compaction conditions affect the capacity of biochar-amended sand filters to treat road runoff. *Sci. Total Environ.*, 139180.
- Gilbreath, A., McKee, L., Shimabuku, I., Lin, D., Werbowksi, L.M., Zhu, X., Grbic, J., Rochman, C., 2019. Multiyear water quality performance and mass accumulation of PCBs, mercury, methylmercury, copper, and microplastics in a bioretention rain garden. *J. Sustain. Water Built Environ.* 5, 04019004. <https://doi.org/10.1061/JSWBAY.0000883>.
- Gu, S., Gruau, G., Malique, F., Dupas, R., Petitjean, P., Gascuel-Oudoux, C., 2018. Drying/rewetting cycles stimulate release of colloidal-bound phosphorus in riparian soils. *Geoderma* 321, 32–41. <https://doi.org/10.1016/j.geoderma.2018.01.015>.
- Hattori, K., Matsushima, D., Demura, K., Kamiya, M., 2020. Particle and pattern discriminant freeze-cleaning method. *J. MicroNanolithography MEMS MOEMS* 19, 044401. <https://doi.org/10.1117/1.JMM.19.4.044401>.
- Henry, H.A.L., 2008. Climate change and soil freezing dynamics: historical trends and projected changes. *Clim. Change* 87, 421–434. <https://doi.org/10.1007/s10584-007-9322-8>.
- Huang, Y., Li, W., Gao, J., Wang, F., Yang, W., Han, L., Lin, D., Min, B., Zhi, Y., Grieger, K., Yao, J., 2021. Effect of microplastics on ecosystem functioning: microbial nitrogen removal mediated by benthic invertebrates. *Sci. Total Environ.* 754, 142133. <https://doi.org/10.1016/j.scitotenv.2020.142133>.
- Keller, A.A., Auset, M., 2007. A review of visualization techniques of biocolloid transport processes at the pore scale under saturated and unsaturated conditions. *Adv. Water Resour., Biol. Processes Porous Media: From the pore scale to the field* 30, 1392–1407. <https://doi.org/10.1016/j.advwatres.2006.05.013>.
- Khalid, N., Aqeel, M., Noman, A., 2020. Microplastics could be a threat to plants in terrestrial systems directly or indirectly. *Environ. Pollut.* 267, 115653. <https://doi.org/10.1016/j.envpol.2020.115653>.
- Körber, Ch., Rau, G., Cosman, M.D., Cravalho, E.G., 1985. Interaction of particles and a moving ice-liquid interface. *J. Cryst. Growth* 72, 649–662. [https://doi.org/10.1016/0022-0248\(85\)90217-9](https://doi.org/10.1016/0022-0248(85)90217-9).
- Koutnik, V.S., Alkidim, S., Leonard, J., DePrima, F., Cao, S., Hoek, E.M.V., Mohanty, S.K., 2021a. Unaccounted microplastics in wastewater sludge: where do they go? *ACS EST Water* 1, 1086–1097. <https://doi.org/10.1021/acsestwater.0c00267>.
- Koutnik, V.S., Borthakur, A., Leonard, J., Alkidim, S., Koydemir, H.C., Tseng, D., Ozcan, A., Ravi, S., Mohanty, S.K., 2022a. Mobility of polypropylene microplastics in stormwater biofilters under freeze-thaw cycles. *J. Hazard. Mater. Lett.* 3, 100048. <https://doi.org/10.1016/j.hazl.2022.100048>.
- Koutnik, V.S., Leonard, J., Alkidim, S., DePrima, F.J., Ravi, S., Hoek, E.M.V., Mohanty, S.K., 2021b. Distribution of microplastics in soil and freshwater environments: global analysis and framework for transport modeling. *Environ. Pollut.* 274, 116552. <https://doi.org/10.1016/j.envpol.2021.116552>.
- Koutnik, V.S., Leonard, J., Glasman, J.B., Brar, J., Koydemir, H.C., Novoselov, A., Bertel, R., Tseng, D., Ozcan, A., Ravi, S., Mohanty, S.K., 2022b. Microplastics retained in stormwater control measures: where do they come from and where do they go? *Water Res.* 210, 118008. <https://doi.org/10.1016/j.watres.2021.118008>.
- Lange, K., Magnusson, K., Viklander, M., Blecken, G.-T., 2021. Removal of rubber, bitumen and other microplastic particles from stormwater by a gross pollutant trap-bioretenion treatment train. *Water Res.* 202, 117457. <https://doi.org/10.1016/j.watres.2021.117457>.
- Leonard, J., Koydemir, H.C., Koutnik, V.S., Tseng, D., Ozcan, A., Mohanty, S.K., 2022. Smartphone-enabled rapid quantification of microplastics. *J. Hazard. Mater. Lett.* 3, 100052. <https://doi.org/10.1016/j.hazl.2022.100052>.
- Li, H., Lu, X., Wang, S., Zheng, B., Xu, Y., 2021. Vertical migration of microplastics along soil profile under different crop root systems. *Environ. Pollut.* 278, 116833. <https://doi.org/10.1016/j.envpol.2021.116833>.
- Li, L., Luo, Y., Li, R., Zhou, Q., Peijnenburg, W.J.G.M., Yin, N., Yang, J., Tu, C., Zhang, Y., 2020. Effective uptake of submicrometre plastics by crop plants via a crack-entry mode. *Nat. Sustain.* 3, 929–937. <https://doi.org/10.1038/s41893-020-0567-9>.
- Li, Shitong, Ding, F., Flury, M., Wang, Z., Xu, L., Li, Shuangyi, Jones, D.L., Wang, J., 2022. Macro- and microplastic accumulation in soil after 32 years of plastic film mulching. *Environ. Pollut.* 300, 118945. <https://doi.org/10.1016/j.envpol.2022.118945>.
- Lin, T., Quan, X., Cheng, P., Li, J., Chen, G., 2020. Interaction between nanoparticles and advancing ice-water interfaces: A molecular dynamics simulation. *Int. J. Heat Mass Transf.* 163, 120412. <https://doi.org/10.1016/j.ijheatmasstransfer.2020.120412>.
- Lutz, N., Fogarty, J., Rate, A., 2021. Accumulation and potential for transport of microplastics in stormwater drains into marine environments, Perth region, Western Australia. *Mar. Pollut. Bull.* 168, 112362. <https://doi.org/10.1016/j.marpolbul.2021.112362>.
- Mohanty, S.K., Saiers, J.E., Ryan, J.N., 2015. Colloid Mobilization in a Fractured Soil during dry-wet cycles: role of drying duration and flow path permeability. *Environ. Sci. Technol.* 49, 9100–9106. <https://doi.org/10.1021/acs.est.5b00889>.
- Mohanty, S.K., Saiers, J.E., Ryan, J.N., 2014. Colloid-facilitated mobilization of metals by freeze-thaw cycles. *Environ. Sci. Technol.* 48, 977–984. <https://doi.org/10.1021/es403698u>.
- Mu, J., Qu, L., Jin, F., Zhang, S., Fang, C., Ma, X., Zhang, W., Huo, C., Cong, Y., Wang, J., 2019. Abundance and distribution of microplastics in the surface sediments from the northern Bering and Chukchi Seas. *Environ. Pollut.* 245, 122–130. <https://doi.org/10.1016/j.envpol.2018.10.097>.
- Nizzetto, L., Futter, M., Langaas, S., 2016. Are agricultural soils dumps for microplastics of urban origin? *Environ. Sci. Technol.* 50, 10777–10779. <https://doi.org/10.1021/acs.est.6b04140>.
- O'Connor, D., Pan, S., Shen, Z., Song, Y., Jin, Y., Wu, W.-M., Hou, D., 2019. Microplastics undergo accelerated vertical migration in sand soil due to small size and wet-dry cycles. *Environ. Pollut.* 249, 527–534. <https://doi.org/10.1016/j.envpol.2019.03.092>.
- Panno, S.V., Kelly, W.R., Scott, J., Zheng, W., McNeish, R.E., Holm, N., Hoellein, T.J., Baranski, E.L., 2019. Microplastic contamination in karst groundwater systems. *Groundwater* 57, 189–196. <https://doi.org/10.1111/gwat.12862>.
- Pauli, J.N., Zuckerberg, B., Whiteman, J.P., Porter, W., 2013. The subnivium: a deteriorating seasonal refugium. *Front. Ecol. Environ.* 11, 260–267. <https://doi.org/10.1890/120222>.
- Piñon-Colin, T., de, J., Rodriguez-Jimenez, R., Rogel-Hernandez, E., Alvarez-Andrade, A., Wakkida, F.T., 2020. Microplastics in stormwater runoff in a semiarid region, Tijuana, Mexico. *Sci. Total Environ.* 704, 135411. <https://doi.org/10.1016/j.scitotenv.2019.135411>.
- Prata, J.C., 2018. Airborne microplastics: consequences to human health? *Environ. Pollut.* 234, 115–126. <https://doi.org/10.1016/j.envpol.2017.11.043>.
- Prata, J.C., da Costa, J.P., Lopes, I., Duarte, A.C., Rocha-Santos, T., 2020. Environmental exposure to microplastics: an overview on possible human health effects. *Sci. Total Environ.* 702, 134455. <https://doi.org/10.1016/j.scitotenv.2019.134455>.
- Rempel, A.W., Worster, M.G., 2001. Particle trapping at an advancing solidification front with interfacial-curvature effects. *J. Cryst. Growth* 223, 420–432. [https://doi.org/10.1016/S0022-0248\(01\)00595-4](https://doi.org/10.1016/S0022-0248(01)00595-4).
- Rempel, A.W., Worster, M.G., 1999. The interaction between a particle and an advancing solidification front. *J. Cryst. Growth* 205, 427–440. [https://doi.org/10.1016/S0022-0248\(99\)00290-0](https://doi.org/10.1016/S0022-0248(99)00290-0).
- Rezaei, M., Riksen, M.J.P.M., Sirjani, E., Sameni, A., Geissen, V., 2019. Wind erosion as a driver for transport of light density microplastics. *Sci. Total Environ.* 669, 273–281. <https://doi.org/10.1016/j.scitotenv.2019.02.382>.
- Rong, H., Li, M., He, L., Zhang, M., Hsieh, L., Wang, S., Han, P., Tong, M., 2022. Transport and deposition behaviors of microplastics in porous media: Co-impacts of N fertilizers and humic acid. *J. Hazard. Mater.* 426, 127787. <https://doi.org/10.1016/j.jhazmat.2021.127787>.
- Saint-Michel, B., Geogelin, M., Deville, S., Pocheau, A., 2017. Interaction of multiple particles with a solidification front: from compacted particle layer to particle trapping. *Langmuir* 33, 5617–5627. <https://doi.org/10.1021/acs.langmuir.7b00472>.
- Samandra, S., Johnston, J.M., Jaeger, J.E., Symons, B., Xie, S., Currell, M., Ellis, A.V., Clarke, B.O., 2022. Microplastic contamination of an unconfined groundwater

- aquifer in Victoria, Australia. *Sci. Total Environ.* 802, 149727 <https://doi.org/10.1016/j.scitotenv.2021.149727>.
- Scheurer, M., Bigalke, M., 2018. Microplastics in swiss floodplain soils. *Environ. Sci. Technol.* 52, 3591–3598. <https://doi.org/10.1021/acs.est.7b06003>.
- Seeley, M.E., Song, B., Passie, R., Hale, R.C., 2020. Microplastics affect sedimentary microbial communities and nitrogen cycling. *Nat. Commun.* 11, 1–10. <https://doi.org/10.1038/s41467-020-16235-3>.
- Seiphooori, A., Ma, X., Arratia, P.E., Jerolmack, D.J., 2020. Formation of stable aggregates by fluid-assembled solid bridges. *Proc. Natl. Acad. Sci.* 117, 3375–3381. <https://doi.org/10.1073/pnas.1913855117>.
- Shang, J., Flury, M., Chen, G., Zhuang, J., 2008. Impact of flow rate, water content, and capillary forces on in situ colloid mobilization during infiltration in unsaturated sediments. *Water Resour. Res.* 44 <https://doi.org/10.1029/2007WR006516>.
- Shangguan, D., Ahuja, S., Stefanescu, D.M., 1992. An analytical model for the interaction between an insoluble particle and an advancing solid/liquid interface. *Metall. Trans. A* 23, 669–680. <https://doi.org/10.1007/BF02801184>.
- Smyth, K., Drake, J., Li, Y., Rochman, C., Van Seters, T., Passeport, E., 2021. Bioretention cells remove microplastics from urban stormwater. *Water Res* 191, 116785. <https://doi.org/10.1016/j.watres.2020.116785>.
- Sørensen, L., Groven, A.S., Hovsbakken, I.A., Del Puerto, O., Krause, D.F., Sarno, A., Booth, A.M., 2021. UV degradation of natural and synthetic microfibers causes fragmentation and release of polymer degradation products and chemical additives. *Sci. Total Environ.* 755, 143170 <https://doi.org/10.1016/j.scitotenv.2020.143170>.
- Spannuth, M., Mochrie, S.G.J., Peppin, S.S.L., Wettlaufer, J.S., 2011. Dynamics of colloidal particles in ice. *J. Chem. Phys.* 135, 224706 <https://doi.org/10.1063/1.3665927>.
- Sun, H., Lei, C., Xu, J., Li, R., 2021. Foliar uptake and leaf-to-root translocation of nanoplastics with different coating charge in maize plants. *J. Hazard. Mater.* 416, 125854 <https://doi.org/10.1016/j.jhazmat.2021.125854>.
- Thompson, J.M.T., Wettlaufer, J.S., 1999. Ice surfaces: macroscopic effects of microscopic structure. *Philos. Trans. R. Soc. Lond. Ser. Math. Phys. Eng. Sci.* 357, 3403–3425. <https://doi.org/10.1098/rsta.1999.0500>.
- Tirpak, A., Afrooz, N., Winston, R.J., Valenca, R., Schiff, K., Mohanty, S.K., 2021. Conventional and Amended Bioretention Soil Media for Targeted Pollutant Treatment: A Critical Review to Guide the State of the Practice. *Water Res* 189, 116648. <https://doi.org/10.1016/j.watres.2020.116648>.
- Tyagi, S., Huynh, H., Monteux, C., Deville, S., 2020. Objects interacting with solidification fronts: Thermal and solute effects. *Materialia* 12, 100802. <https://doi.org/10.1016/j.mtla.2020.100802>.
- Viaroli, S., Lancia, M., Re, V., 2022. Microplastics contamination of groundwater: current evidence and future perspectives. A review. *Sci. Total Environ.* 824, 153851 <https://doi.org/10.1016/j.scitotenv.2022.153851>.
- Waldschläger, K., Schüttrumpf, H., 2020. Infiltration behavior of microplastic particles with different densities, sizes, and shapes—from glass spheres to natural sediments. *Environ. Sci. Technol.* 54, 9366–9373. <https://doi.org/10.1021/acs.est.0c01722>.
- Werbowski, L.M., Gilbreath, A.N., Munno, K., Zhu, X., Grbic, J., Wu, T., Sutton, R., Sedlak, M.D., Deshpande, A.D., Rochman, C.M., 2021. Urban stormwater runoff: a major pathway for anthropogenic particles, black rubbery fragments, and other types of microplastics to urban receiving waters. *ACS EST Water* 1, 1420–1428. <https://doi.org/10.1021/acsestwater.1c00017>.
- Zhang, Q., Hassanizadeh, S.M., Liu, B., Schijven, J.F., Karadimitriou, N.K., 2014. Effect of hydrophobicity on colloid transport during two-phase flow in a micromodel. *Water Resour. Res.* 50, 7677–7691. <https://doi.org/10.1002/2013WR015198>.
- Zhou, D., Cai, Y., Yang, Z., 2022. Key factors controlling transport of micro- and nanoplastic in porous media and its effect on coexisting pollutants. *Environ. Pollut.* 293, 118503 <https://doi.org/10.1016/j.envpol.2021.118503>.
- Zumstein, M.T., Schintlmeister, A., Nelson, T.F., Baumgartner, R., Wobken, D., Wagner, M., Kohler, H.-P.E., McNeill, K., Sander, M., 2018. Biodegradation of synthetic polymers in soils: Tracking carbon into CO₂ and microbial biomass. *Sci. Adv.* 4 <https://doi.org/10.1126/sciadv.aas9024> eaa9024.